© 2016. Published by The Company of Biologists Ltd | Development (2016) 143, 2664-2676 doi:10.1242/dev.134759

RESEARCH ARTICLE

Drosophila dany is essential for transcriptional control and nuclear architecture in spermatocytes

Martina Trost‡, Ariane C. Blattner‡, Stefano Leo* and Christian F. Lehner§

ABSTRACT

The terminal differentiation of adult stem cell progeny depends on transcriptional control. A dramatic change in gene expression programs accompanies the transition from proliferating spermatogonia to postmitotic spermatocytes, which prepare for meiosis and subsequent spermiogenesis. More than a thousand spermatocyte-specific genes are transcriptionally activated in early *Drosophila* spermatocytes. Here we describe the identification and initial characterization of *dany*, a gene required in spermatocytes for the large-scale change in gene expression. Similar to tMAC and tTAFs, the known major activators of spermatocyte-specific genes, *dany* has a recent evolutionary origin, but it functions independently. Like *dan* and *danr*, its primordial relatives with functions in somatic tissues, *dany* encodes a nuclear Psq domain protein. Dany associates preferentially with euchromatic genome regions. In *dany* mutant spermatocytes, activation of spermatocyte-specific genes and silencing of non-spermatocyte-specific genes are severely compromised and the chromatin no longer associates intimately with the nuclear envelope. Therefore, as suggested recently for Dan/Danr, we propose that Dany is essential for the coordination of change in cell type-specific expression programs and large-scale spatial chromatin reorganization.

KEY WORDS: Chromatin, Transcription, Spermatocytes, Differentiation, Meiosis

INTRODUCTION

Meiotic sex has a deep evolutionary origin in basal eukaryotes. While meiosis has generally remained well conserved, most other aspects of sexual reproduction have diverged rapidly. In animals that differentiate a male and a female gender, male-biased genes and in particular those expressed in the germline are affected by turnover and sequence divergence that is significantly faster than in other gene classes (Parsch and Ellegren, 2013). Analyses in *Drosophila melanogaster* spermatocytes have provided some of the most striking evidence for rapid evolutionary dynamics even in key elements of transcriptional networks with numerous interactions.

The comparison of different tissues in adult *D. melanogaster* has clearly revealed that the number of genes with an expression apparently restricted to a single tissue is maximal in the case of testis (Andrews et al., 2000; Chintapalli et al., 2007; Dorus et al., 2006; Vibranovski et al., 2009; Zhao et al., 2010). The large majority of these, as well as of the testis-biased genes, are transcribed in spermatocytes, i.e. in germline cells during a growth phase between the last mitotic division and the onset of the meiotic divisions and spermiogenesis. The transcription of more than 1000 of these genes depends on the function of the testis meiotic arrest complex (tMAC) (Beall et al., 2007; White-Cooper, 2010). tMAC is a testis-specific variant of the MIP/dREAM/SynMuvB complex, a widely conserved somatic transcriptional regulator (Sadasivam and DeCaprio, 2013). tMAC contains subunits encoded by testis-specific paralogs (*aly*, *tomb*) that are only present within the genus *Drosophila*. They were identified based on a characteristic loss-of-function phenotype in which the testes fill up with spermatocytes failing to enter meiotic divisions and postmeiotic differentiation (Jiang et al., 2007; Lin et al., 1996; White-Cooper et al., 2000). Several genes of comparably recent origin and with similar mutant phenotypes (*topi*, *comr*, *achi*, *vis*) encode proteins interacting with tMAC (Ayyar et al., 2003; Jiang and White-Cooper, 2003; Perezgasga et al., 2004; Wang and Mann, 2003). A second protein complex of paramount importance for spermatocyte-specific transcription is formed by testis-specific TATA-binding protein (TBP)-associated factors (tTAFs) in the genus *Drosophila* (Chen et al., 2005; Hiller et al., 2004; Li et al., 2009). The tTAF genes [*can*, *mia*, *nht*, *rye* (*Taf12L* – FlyBase), *sa*] were also identified based on their mutant phenotype, which is slightly milder than that associated with tMAC loss.

Here we describe the identification of *dany*, yet another gene with a recent evolutionary origin and an essential role in spermatocyte-specific gene expression. *dany* is most similar to the *Drosophila* genes *distal antenna* (*dan*) and *distal antenna-related* (*danr*). Dan and Danr have recently been implicated in the control of neuroblast competence in *Drosophila* embryos, where they inhibit the repositioning of crucial target genes into repressive chromatin associated with the nuclear lamina (Kohwi et al., 2013). Similarly, Dany is required not only for cell type-specific gene expression in spermatocytes but also for normal association of chromatin with the nuclear envelope.

RESULTS

dany, a young gene related to *dan* and *danr*

To identify novel genes that might provide meiosis-specific functions, we searched for *Drosophila* genes expressed predominantly or exclusively in ovaries and testes using various data sources (Brown et al., 2014; Chintapalli et al., 2007; Gan et al., 2010; Graveley et al., 2011; Vibranovski et al., 2009). For further characterization, we targeted candidate genes by transgenic RNA interference (RNAi) in spermatocytes. In the case of the previously uncharacterized gene *CG30401*, knockdown resulted in male sterility. Therefore, we undertook a more detailed characterization of this gene.

CG30401 encodes a protein with a single N-terminal Psq motif (Fig. 1A,B) (Siegmund and Lehmann, 2002). This motif of ∼50 amino acids contains a helix-turn-helix domain (Fig. 1B) and is

Institute of Molecular Life Sciences (IMLS), University of Zurich, Zurich 8057, Switzerland.
*Present address: Genomic Research Laboratory, Division of Infectious Diseases, University of Geneva Hospitals, Geneva 1211, Switzerland.
‡These authors contributed equally to this work

§Author for correspondence (christian.lehner@imls.uzh.ch)

C.F.L., 0000-0003-0185-6049

Received 4 January 2016; Accepted 3 June 2016

Development (2016) 143, 2664-2676 doi:10.1242/dev.134759

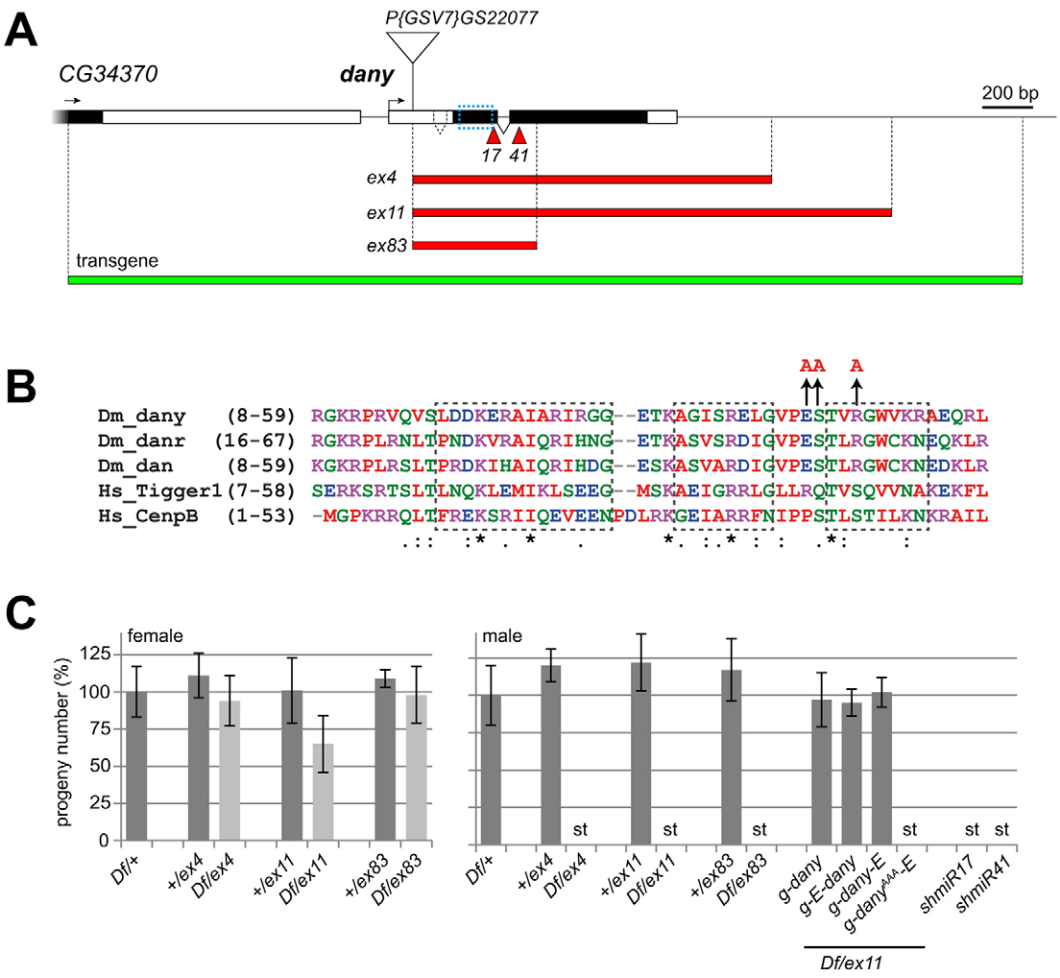

Fig. 1. Psq gene family member *dany* is required for male fertility. (A) Scheme illustrating *Drosophila dany* gene structure, alleles and transgenes. Black boxes represent coding regions. The Psq motif region is indicated by the blue dotted box. Red arrowheads indicate regions targeted by RNAi transgenes *UAS-V20dany*^{shmiR17} (*17*) and *UAS-W20dany*^{shmiR41} (*41*). Red bars indicate regions deleted in the alleles *dany*^{ex4} (*ex4*), *dany*^{ex11} (*ex11*) and *dany*^{ex83} (*ex83*), which were isolated as imprecise excisions after mobilization of the transposon insertion *P{GSV7}GS22077* (triangle). The green bar indicates the region present in the transgenes *g-dany*, *g-EGFP-dany*, *g-dany-EGFP* and *g-dany*^{AAA}*-EGFP*. (B) Alignment of the Psq motif regions in Dany, Danr, Dan, human Tigger 1 transposase and CENPB. Dashed boxes indicate regions that are helical within CENPB (Tanaka et al., 2001). Three codons for amino acids at positions predicted to interact with DNA according to the structure of a DNA–CENPB complex (Tanaka et al., 2001) were mutated to alanine codons (E45A, S46A and R49A) in the *g-dany*^{AAA}*-EGFP* transgene. Symbols below the alignment indicate sequence identity (asterisk), high similarity (:) and low similarity (.). (C) Fertility assays, showing the mean fertility of females (left) and males (right) of genotypes *Df(2R)BSC802* (*Df*), *dany*^{ex4} (*ex4*), *dany*^{ex11} (*ex11*), *dany*^{ex83} (*ex83*), *g-dany*, *g-EGFP-dany* (*g-E-dany*), *g-dany-EGFP* (*g-dany-E*), *g-dany*^{AAA}*-EGFP* (*g-dany*^{AAA}*-E*), *bam-GAL4-VP16>UAS-V20dany*^{shmiR17} (*shmiR17*) and *bamGAL4-VP16>UAS-W20dany*^{shmiR41} (*shmiR41*). The number of progeny obtained from *Df(2R)BSC802*/+ was set to 100%. Error bars indicate s.d. Absence or knockdown of *dany* gene function had little effect in females but resulted in complete sterility (st) in males. Dark and light gray bars indicate one or no functional *dany* gene copy, respectively.

present in a family of proteins that includes transposases and the centromere protein CENPB. The Psq motif of *CG30401* is most similar to that of the *Drosophila* gene *dan* and its tandem duplication *danr*. Whereas *dan*/*danr* orthologs are readily detectable throughout the insect lineage, *CG30401* orthologs are restricted to the genus *Drosophila*. Reflecting its young evolutionary origin, *dany* will be used as name for *CG30401*. The similarity between *dany* and *dan*/*danr* is restricted to the Psq motif. *dan*/*danr* expression occurs in various somatic tissues during development but not in gonads. By contrast, *dany* transcripts appear to be restricted to ovaries and testis (Brown et al., 2014; Chintapalli et al., 2007; Graveley et al., 2011).

dany is required in male germ cells for progression beyond the spermatocyte stage

To evaluate *dany* function, we generated null mutations by isolating imprecise excision events after mobilizing the transposon *P{GSV7}GS22077* (Fig. 1A). Molecular characterization of *dany*^{ex4}, *dany*^{ex11} and *dany*^{ex83} revealed deletions removing substantial parts or the entire gene. These alleles were crossed over a deficiency *Df(2R)BSC802* that deletes the *dany* region. *dany*^{ex} hemizygous adults eclosed with the expected Mendelian frequency free of obvious morphological abnormalities. Female fertility was at most slightly reduced (Fig. 1C). However, males were sterile (Fig. 1C). A transgene (*g-dany*) made with a genomic fragment containing only *dany* (Fig. 1A) completely restored male fertility in *dany*^{ex11}*/Df(2R)BSC802* (Fig. 1C). We conclude that *dany* is required for male fertility.

To assess whether *dany* function is required in the germline, we expressed *UAS-V20dany*^{shmiR17} specifically in early spermatocytes. This also caused male sterility (Fig. 1A,C). The same result was obtained with *UAS-W20dany*^{shmiR41}, which targets a different region within *dany* (Fig. 1A,C). We conclude that *dany* function is required in spermatocytes.

Development (2016) 143, 2664-2676 doi:10.1242/dev.134759

For further characterization of the defects resulting from loss of *dany*, testes were dissected. Whereas testes from heterozygous deficient males (+/*Df(2R)BSC802*) were of wild-type appearance, including prominent sperm tail bundles, those from *dany* null males ($dany^{ex4}$, $dany^{ex11}$ or $dany^{ex83}$/*Df(2R)BSC802*) were clearly abnormal (Fig. 2; data not shown). These testes were slightly smaller and did not contain sperm tail bundles. Instead, they were full of spermatocytes, which are normally confined to the distal third of the testis tube. *g-dany* restored a wild-type appearance to testes in *dany* null mutant males (Fig. 3A). By contrast, testes after spermatocyte-specific *dany* knockdown were very similar to *dany* null mutant testes (Fig. 2; data not shown). We conclude that *dany* is required for normal spermatogenesis to proceed beyond the spermatocyte stage.

Dany is a nuclear protein that associates with chromatin

To characterize the pattern of *dany* expression, we generated transgenic lines that express Dany fused to EGFP under the control of the *dany* cis-regulatory region (*g-EGFP-dany* and *g-dany-EGFP*). To determine whether these transgenes can functionally replace *dany*, they were crossed into a *dany* null mutant background ($dany^{ex11}$/*Df(2R)BSC802*). The resulting males were fully fertile (Fig. 1C). We conclude that the EGFP fusion proteins are functional and expressed in a pattern that restores male fertility in *dany* null mutants.

To analyze the pattern of *dany* expression during spermatogenesis, testes were dissected from males with either *g-EGFP-dany* or *g-dany-EGFP* in a *dany* null background (Fig. 3A). Nuclear EGFP signals were first observed in young spermatocytes. The signals persisted throughout the spermatocyte stages, but faded rapidly during the postmeiotic stages. To study subcellular localization, testis squash preparations were made using *dany* null males rescued by *g-dany-EGFP* (Fig. 3B). In early spermatocytes (stages S1-S3) (Cenci et al., 1994), EGFP signals were mostly diffuse throughout the nucleus. In mid spermatocytes (S4, S5), EGFP signals were enriched on chromosome territories (Cenci et al., 1994). A prominent enrichment in the nucleolus became apparent in late spermatocytes (late S5 and S6), as confirmed by double labeling with anti-Fibrillarin, which marks a nucleolar subcompartment (Fig. 3C). At high magnification it was also evident that the enrichment in chromosome territories occurs primarily at their periphery and less within their central heterochromatic regions as characterized by the brightest DNA staining. EGFP-Dany was localized similarly to Dany-EGFP, except for somewhat lower levels of diffuse nuclear signals (Fig. 3C, Fig. S1).

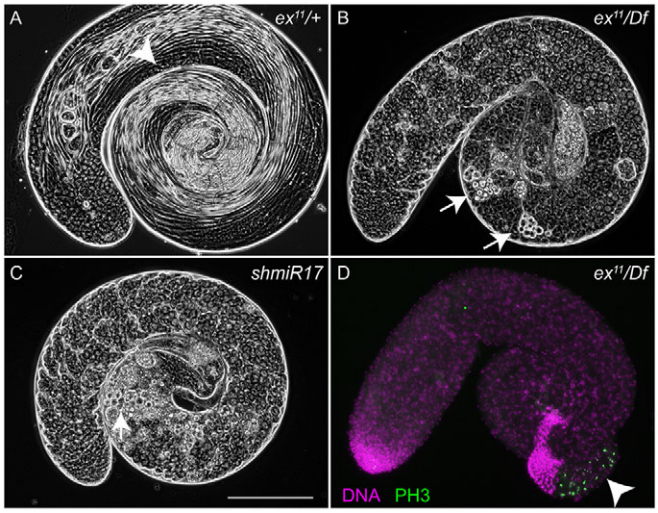

Fig. 2. *dany* is required for normal spermatogenesis to proceed beyond the spermatocyte stage. Phase contrast images (A-C) of testes isolated from $dany^{ex11}$/*Df(2R)BSC802*, where *dany* function is completely lacking (B; ex^{11}/*Df*), and from *bam-GAL4-VP16>UAS-V20dany*^{shmiR17}, where *dany* knockdown occurs specifically in early spermatocytes (C; *shmiR17*), reveal an accumulation of spermatocytes and a lack of spermatid bundles, whereas the latter are clearly apparent in control testes from $dany^{ex11}$/+ (A; ex^{11}/+). At the base of testes from *dany* mutant (B) or knockdown (C) males, rare conspicuous spermatocyte cysts were observed (arrows) presumably representing degenerating cysts rather than cysts that have entered into aberrant meiotic divisions, which were also detected in this proximal region (arrowhead) by anti-phospho-histone H3 immunolabeling (PH3) and DNA staining (D; ex^{11}/*Df*). For comparison, the region where cysts are normally observed during meiotic divisions is indicated in the control testis (A, arrowhead). Scale bar: 200 µm.

The subcellular localization of the Dany EGFP fusions in spermatocytes suggested that a fraction of Dany is chromatin associated. To explore this further, UASt transgenes were generated for targeted expression in larval salivary glands, which have large polytene chromosomes. However, initial experiments revealed that ectopic *dany* expression is highly toxic, not just in salivary glands but also in other somatic tissues. Various GAL4 drivers (*Act5C*, *en*, *ey*, *GMR*, *sev*) in combination with *UASt-dany*, *UASt-EGFP-dany* or *UASt-dany-EGFP* caused complete larval or pupal lethality in most cases. In combination with a salivary gland-specific GAL4 driver (F4), larvae developed that did not contain recognizable salivary glands. By contrast, expression of these transgenes in testis with *bam-GAL4-VP16* did not have toxic effects. *bam-GAL4-VP16*-driven *UASt-EGFP-dany* expression was unable to restore fertility in *dany* null males, presumably because expression clearly did not perdure to the late spermatocyte stages (data not shown), as is observed with transgenes under control of the *dany* cis-regulatory region. These results emphasize that precise control of *dany* expression is crucial. For normal spermatogenesis, *dany* needs to be expressed in spermatocytes for an appropriate period. Moreover, detrimental ectopic expression in somatic tissues must be prevented.

To minimize confounding toxicity during localization studies in salivary glands, *UASt-EGFP-dany* was expressed only briefly by means of the Gal4/Gal80^{ts} system. After 4 h of induction at 29°C, EGFP-Dany was detectable in salivary gland nuclei of third instar larvae (Fig. 3D). EGFP-Dany was not observed when the temperature shift was omitted or when GAL4 and UASt transgenes were not both present (data not shown). Salivary glands were of normal appearance after 4 h of EGFP-Dany expression. Interestingly, EGFP-Dany was enriched on polytene chromosomes, where it was preferentially associated with interbands that have lower DNA staining (Fig. 3D). In conclusion, Dany can associate with chromatin with a preference for euchromatic regions.

In the case of Dan and Danr, there is no direct evidence for DNA binding so far. However, this has been demonstrated for more distant relatives such as human CENPB and various transposases. Structural analyses have revealed several residues within the Psq motif of CENPB that contact the bound DNA (Tanaka et al., 2001). To evaluate the involvement of corresponding residues within the Psq motif of Dany, we generated a mutant transgene, *g-dany*^{AAA}*-EGFP*, that encodes a variant with three alanine residues in place of those in the wild-type protein (Fig. 1B). Complementation tests in a *dany* null background ($dany^{ex11}$/*Df(2R)BSC802*) revealed that this triple A version is not fully functional. It did not restore male fertility (Fig. 1C). However, the triple A mutation did not completely abolish *dany* function. When *g-dany*^{AAA}*-EGFP* was present in the

Development (2016) 143, 2664-2676 doi:10.1242/dev.134759

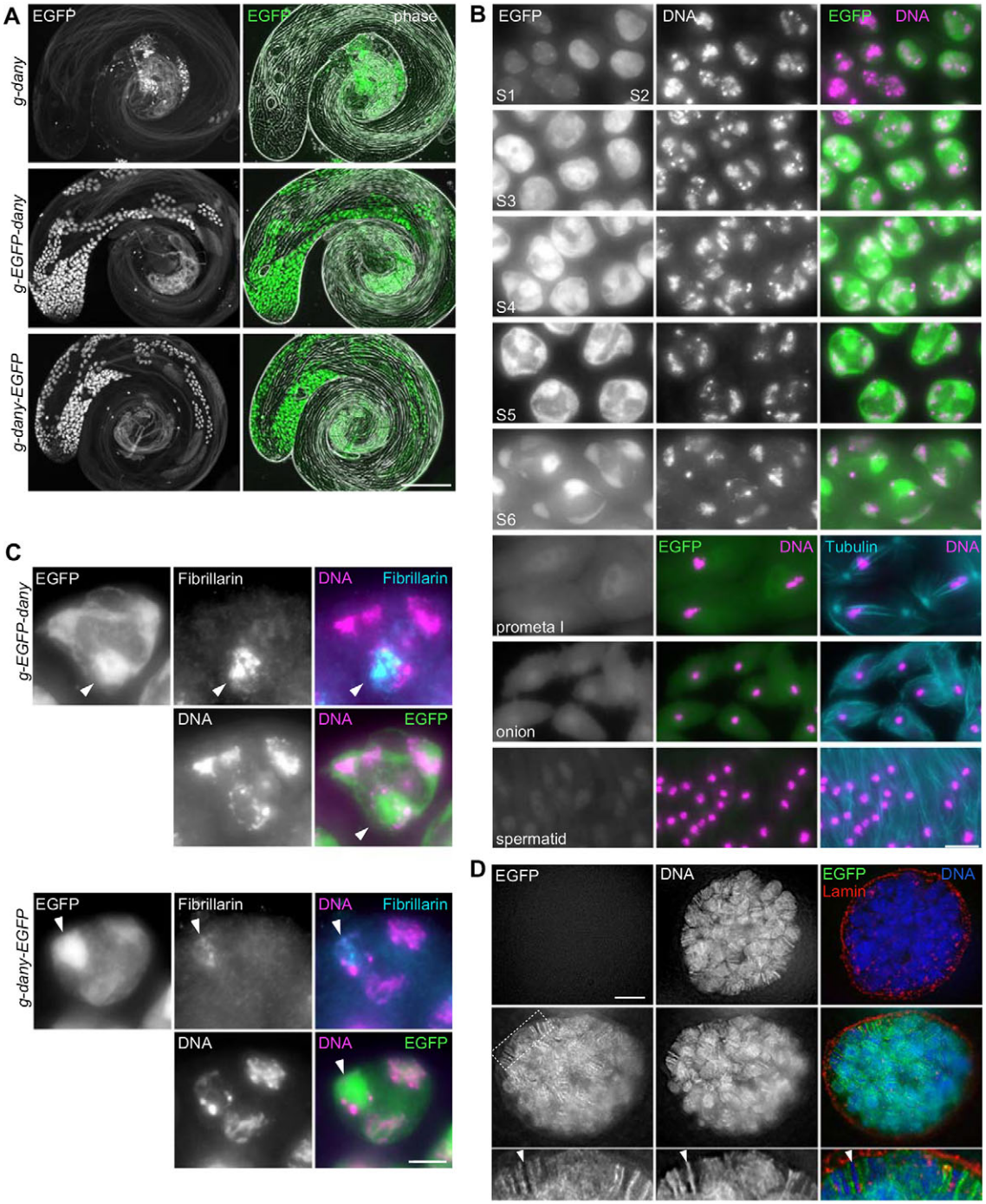

Fig. 3. Expression pattern and subcellular localization of Dany. (A) Testes isolated from *dany* null mutants (*dany*^{ex11}/*Df(2R)BSC802*) carrying one copy of the indicated transgenes (*g-dany*, *g-EGFP-dany* or *g-dany-EGFP*) revealed the functionality of these transgenes and that *dany* is expressed during the spermatocyte stages. (B) Cyst regions after squash preparations of testis from *dany*^{ex11}/*Df(2R)BSC802* carrying *g-dany-EGFP* revealed accumulation and subnuclear distribution of Dany-EGFP during the indicated stages. In addition to EGFP signals and DNA staining, anti-Tubulin labeling is displayed in the case of meiotic and early postmeiotic stages. (C) High-magnification views of S5 spermatocytes from *dany*^{ex11}/*Df(2R)BSC802* with either *g-EGFP-dany* (top) or *g-dany-EGFP* (bottom) after double labeling with anti-Fibrillarin and a DNA stain indicate that Dany EGFP fusions are enriched over chromosome territories and most prominently in the nucleolus (arrowheads). (D) Salivary gland nuclei from *esg-GAL4, tub-GAL80*^{ts} larvae carrying *UASt-EGFP-dany* either before (top row) or after (lower rows) a 4 h temperature shift from 18°C to 29°C are displayed after staining with anti-Lamin and a DNA stain. The boxed region is shown at higher magnification beneath and reveals that chromosomal EGFP-Dany is enriched in interbands and is scarce or absent in bands (arrowheads). Scale bars: 200 µm in A; 10 µm in B,D; 5 µm in C.

dany null mutants, spermatogenesis progressed beyond the spermatocyte stages to a considerable extent. Bundles of spermatids with elongated sperm tails were abundant (Fig. S2A), in contrast to *dany* null mutants (Fig. 2). Dany^{AAA}-EGFP expression and localization in spermatocytes appeared to be normal (Fig. S2A,B). However, DNA staining revealed strong nuclear abnormalities in postmeiotic stages (Fig. S2C), and seminal vesicles were always devoid of motile sperm. We conclude that the

Development (2016) 143, 2664-2676 doi:10.1242/dev.134759

triple A mutation in the Psq motif of Dany causes a partial loss of function.

The normal spermatocyte transcription program depends on *dany* function

The expression program and mutant phenotype observed for *dany* corresponded to those of 'meiotic arrest' genes (White-Cooper, 2010). The majority of these genes encode tTAFs or tMAC components. To evaluate whether a loss of *dany* causes similar transcriptome changes as tTAF or tMAC mutations, we probed microarrays with RNA isolated from testes of control males and of males lacking either *dany*, *aly*, *sa* or *topi* function. Hierarchal clustering of the data revealed highest similarities between biological replicates, as expected (Fig. 4A). Moreover, also in accord with expectations, the samples from the two analyzed tMAC mutants (*aly* and *topi*) were more similar to each other than to the tTAF mutant *sa*. The *sa* samples were slightly more similar to the control than were the *dany* samples.

The comparison of control and *dany* mutants (Fig. 4B) revealed a considerable fraction of genes with differential transcript levels (14% after filtering for probes with a change in signal intensity higher than 4-fold and an FDR-adjusted *P*-value less than 0.05). Compared with the control, ∼1000 genes had lower ('*dany*Down') and 1600 genes had higher ('*dany*Up') transcript levels in the mutant. In controls, the *dany*Down genes were 12-fold more strongly expressed overall than the *dany*Up genes (Fig. 4C). Moreover, the *dany*Down set predominantly contained genes with testis-specific or testis-biased expression, whereas such testis genes were strongly depleted in the *dany*Up gene set (Fig. S3A). These results suggest that Dany is important not just for the transcriptional activation of spermatocyte-specific genes but also for the repression of genes that function specifically in other tissues.

Our finding that more genes had increased rather than decreased transcript levels in *dany* mutants indicated that *dany* functions in a manner distinct from tMAC and tTAFs. These were reported to be required primarily for transcriptional activation of spermatocyte-specific genes (Doggett et al., 2011; Lu and Fuller, 2015; White-Cooper and Caporilli, 2013). Our direct comparison of transcriptome changes in *dany* mutants with those in *sa*, *aly* and *topi* mutants confirmed this notion (Fig. 4D-F). In general, those transcripts that were increased in *dany* mutants relative to the control were not also increased in the other mutants (Fig. 4D). However, transcripts that were decreased in *dany* mutants were generally also decreased in the other mutants (Fig. 4E). The greatest number of genes showing decreased transcript levels and the strongest decreases were observed in *aly* and *topi* mutants (Fig. 4F; data not shown), consistent with previous analyses (Doggett et al., 2011; Lu and Fuller, 2015). Most of these *aly*/*topi*-dependent genes also had decreased transcript levels in *sa* mutants, although in general to a more modest extent (Fig. 4E, Fig. S3B,C). In addition, most of these

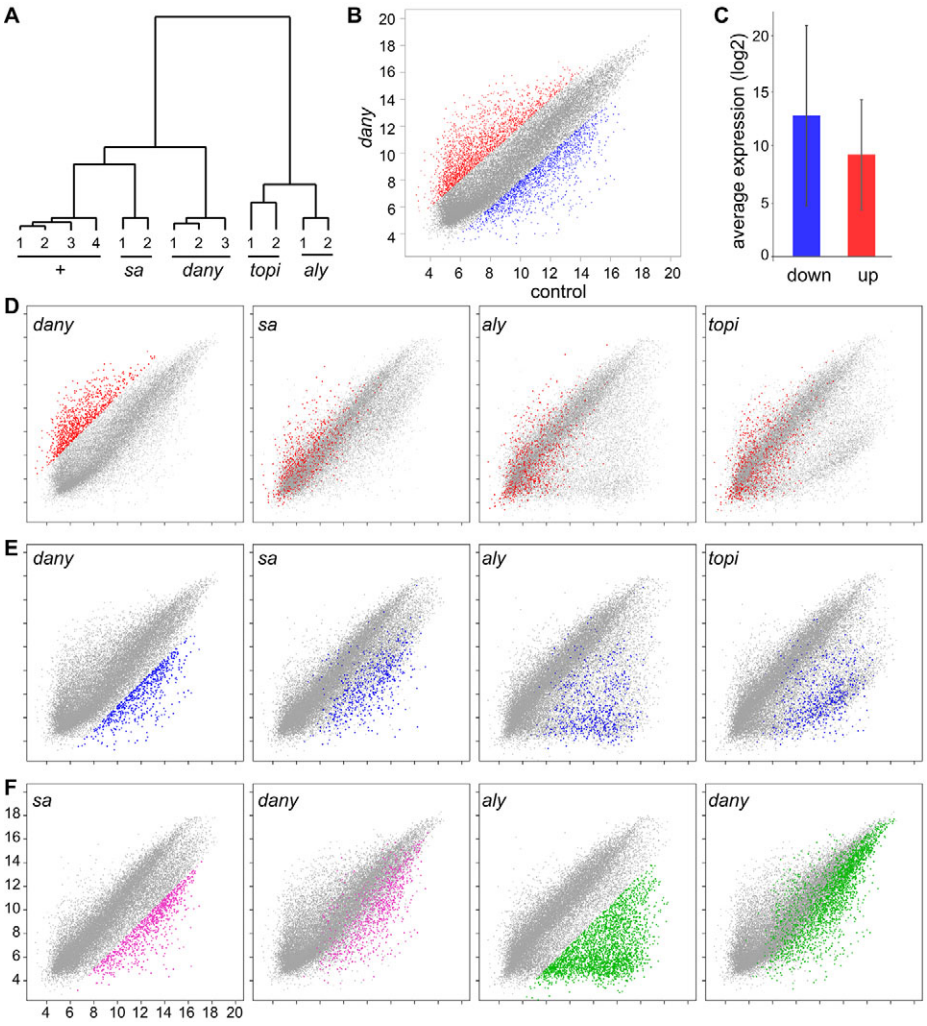

Fig. 4. Dysregulated transcription program in *dany* mutant testis. RNA samples isolated from testis of +/*Df(2R)BSC802* controls (+) or males lacking function of *dany* (*dany*^{ex11}/*Df(2R)BSC802*) or the meiotic arrest genes *sa*, *aly* or *topi* were analyzed using gene expression microarrays. (A) Hierarchical clustering was used for comparison of the different genotypes and the biological replicates of each genotype. (B) Scatter plot comparing $\log_2$ transformed signal intensities obtained with *dany* mutant (*dany*^{ex11}/*Df(2R)BSC802*) and control (+/*Df(2R)BSC802*) testis samples. Probes with signals that were at least 4-fold stronger in *dany* mutants are shown in red (up; *n*=2195, 8.1% of all probes). Conversely, probes with signals that were at least 4-fold weaker in *dany* mutants are shown in blue (down; *n*=1521, 5.7% of all probes). (C) Average signal intensity in control (+/*Df(2R)BSC802*) of all the probes that are at least 4-fold weaker or stronger in *dany* mutants (mean±s.e.). Genes that are downregulated in *dany* mutants are strongly expressed in normal testis, whereas genes that are derepressed in *dany* mutants have very low expression in normal testis. The difference in the average transcript levels of the down and up probes was highly significant (*P*<0.00001, *t*-test). (D-F) Scatter plots comparing $\log_2$ transformed signal intensities in control (always *x*-axis) and the indicated mutants (always *y*-axis). (D) Analysis of *dany*Up probes (red; at least 8-fold; 996) in *sa*, *aly* and *topi* mutants. (E) Analysis of *dany*Down probes (blue; at least 8-fold; 596) in *sa*, *aly* and *topi* mutants. (F) Analysis of *sa*Down probes (magenta; at least 8-fold; 107) in *dany* mutants and of *aly*Down probes (green; at least 8-fold; 1557) in *dany* mutants.

Development (2016) 143, 2664-2676 doi:10.1242/dev.134759

genes also had decreased transcript levels in *dany* mutants, where the decreases were usually slightly less severe than in the *sa* mutants (Fig. 4E, Fig. S3B,C).

dany and other meiotic arrest genes do not cross-regulate each other

The transcriptome changes observed in *dany* mutants were distinct from those caused by loss of tTAF and tMAC function, suggesting that *dany* might work independently of these transcriptional activators of spermatocyte-specific genes. Supporting this notion, loss of *dany* did not affect the transcript levels of tTAF and tMAC genes and, vice versa, *dany* transcript levels were not changed in *aly*, *topi* and *sa* mutants (Fig. 5A). Reassuringly, however, *dany* transcript levels were abolished in the *dany* null mutants, as expected (Fig. 5A).

For further analysis of potential functional relations between tTAFs, tMAC and *dany*, we performed microscopic analyses. In contrast to tMAC proteins, which accumulate on spermatocyte chromatin but not in the nucleolus (Doggett et al., 2011; Jiang et al., 2007), tTAF proteins including Sa accumulate primarily in the nucleolus (Chen et al., 2005). As nucleolar enrichment of Dany EGFP fusions had been observed as well (Fig. 3C), we analyzed the colocalization of Sa and Dany in further detail. Double labeling of *g-EGFP-dany* spermatocytes with anti-Sa revealed that the two proteins are not strictly colocalized at stage S5 (Fig. 5B). As expected (Chen et al., 2005), Sa was detected primarily in the nucleolus. In addition, weak nuclear signals that presumably represent Y loops were also obtained with anti-Sa. As these non-nucleolar signals were not observed in *sa-EGFP* testis (see below), they most likely reflect non-specific anti-Sa staining. In comparison to Sa, the presence of EGFP-Dany in chromosome territories outside of the nucleolus was far more prominent. Moreover, subcellular localization was even more distinct at the onset of *sa* and *dany* expression in early spermatocytes (Fig. 5C). Whereas Sa-EGFP accumulation in the nucleolus occurred already at the onset of expression, nucleolar enrichment of Dany EGFP fusions was observed only in late spermatocytes.

To address whether *sa* expression and localization depended on *dany* function, we analyzed Sa-EGFP in *dany* null mutants. We did not detect an abnormal Sa-EGFP behavior in *dany* mutants (Fig. 5C). Loss of *dany* function also did not affect expression and subcellular localization of the *can* product, another tTAF (Chen et al., 2005), which we studied with the help of a functional *can-myc* transgene (Fig. S4A). tTAFs have been proposed to function in part by sequestering Polycomb (Pc), a core component of the PRC1 repressive chromatin complex (Steffen and Ringrose, 2014), in the nucleolus (Chen et al., 2005, 2011; White-Cooper and Caporilli, 2013), although this notion has been challenged recently (El-Sharnouby et al., 2013). We were unable to detect abnormalities in the expression and localization of Pc-EGFP in *dany* mutants (Fig. S4B). Nevertheless, the list of genes that were strongly derepressed in *dany* mutant testis was significantly enriched for genes that had been identified as Pc targets previously in several independent ChIP experiments (Table S1).

Beyond the above finding that *dany* function is dispensable for the expression and nucleolar localization of tTAFs such as Sa and Can, we analyzed whether, conversely, *sa* might be required for Dany accumulation or localization. In addition, with analyses in *aly* and *topi* mutants, we addressed whether tMAC function is required for Dany accumulation or localization. *g-EGFP-dany* and *g-dany-EGFP* were therefore crossed into males with transheterozygous combinations of strong alleles that are thought to abolish the function of *sa*, *aly* or *topi* completely (Hiller et al., 2004; Perezgasga et al., 2004; White-Cooper et al., 2000). Expression of EGFP-tagged Dany was still observed in mutant testis, starting in early spermatocytes as in wild type, and reaching apparently normal levels. Intranuclear localization, however, was affected in mutant testis. The enrichment of the Dany EGFP fusions that eventually occurs during wild-type spermatogenesis within chromosome territories and nucleolus in late spermatocytes was largely abolished in the mutants (Fig. 5D; data not shown). This abnormal localization of Dany in late spermatocytes might reflect a failure of normal spermatocyte differentiation in the absence of tMAC and tTAFs, and hence possibly secondary consequences of the mutations in *sa*, *aly* and *topi*. Importantly, however, *dany* expression clearly does not depend on tMAC and tTAFs. Vice versa, Dany does not function by allowing expression of tMAC and tTAFs.

In the context of our microscopy analyses of EGFP-tagged Dany, we noticed a surprisingly abrupt transition from EGFP-positive to EGFP-negative spermatocytes within the proximal part of *sa*, *aly* and *topi* mutant testes (data not shown). Those aspects of the spermatocyte differentiation program that bring about the postmeiotic disappearance of Dany during normal spermatogenesis might therefore still occur in these mutants. Alternatively, the eventual disappearance of Dany EGFP fusions in mutant testes might reflect a degeneration process rather than an aspect of normal spermatogenesis. However, in *dany* mutant spermatocytes, at least some differentiation processes appear to progress beyond the spermatocyte stage. In the proximal region of *dany* mutant testes, nucleolar Sa-EGFP disappeared abruptly concomitant with enhanced chromatin condensation, nuclear lamina depolymerization and formation of abnormal spindles (data not shown), suggesting the occurrence of meiotic divisions. Anti-phospho-histone H3, a widely used M-phase marker, labeled some spermatocytes close to the terminal epithelium in most *dany* mutant testes (in 13 of 16 analyzed testes) (Fig. 2D). To analyze these meiotic divisions further, we crossed the centriole marker EYFP-Asl into *dany* mutant spermatocytes and performed double labeling with anti-tubulin (Fig. 5E). This staining confirmed that *dany* mutant spermatocytes eventually enter meiotic divisions. Although spindles were readily observed, they lacked normal centrosomes with regular numbers of centrioles at the spindle poles. Moreover, they were often kinked or multipolar. Anaphase figures were never observed, indicating that the chromosomes did not attach normally to spindle fibers. We conclude that loss of *dany* function does not result in a complete arrest before entry into meiotic divisions, as characteristically reported in the case of mutations in tTAF and tMAC genes (White-Cooper, 2010).

Dany is required for normal association of chromatin with the nuclear envelope

To identify early consequences of *dany* loss, we analyzed spermatocyte morphology at the stages when *dany* expression normally starts. As *dany* is required for the realization of a normal transcriptional program, we examined the distribution of DNA within spermatocyte nuclei as delimited by Lamin (Lam) staining. Control and *dany* mutant spermatocytes were undistinguishable at stage S2 (not shown), but differences were clearly apparent at stage S3 (Fig. 6A). In controls (*w*, as well as $dany^{ex11}$/*Df(2R)BSC802* rescued by one copy of *g-dany*), the forming chromosome territories seemed as if pulling the nuclear lamina around them, resulting in conspicuous nuclear lamina deformations. By contrast, *dany* mutants ($dany^{ex11}$/*Df(2R)BSC802*) had a nuclear lamina that was balloon-like, lacking deformations correlated with chromatin distribution. At the same

Development (2016) 143, 2664-2676 doi:10.1242/dev.134759

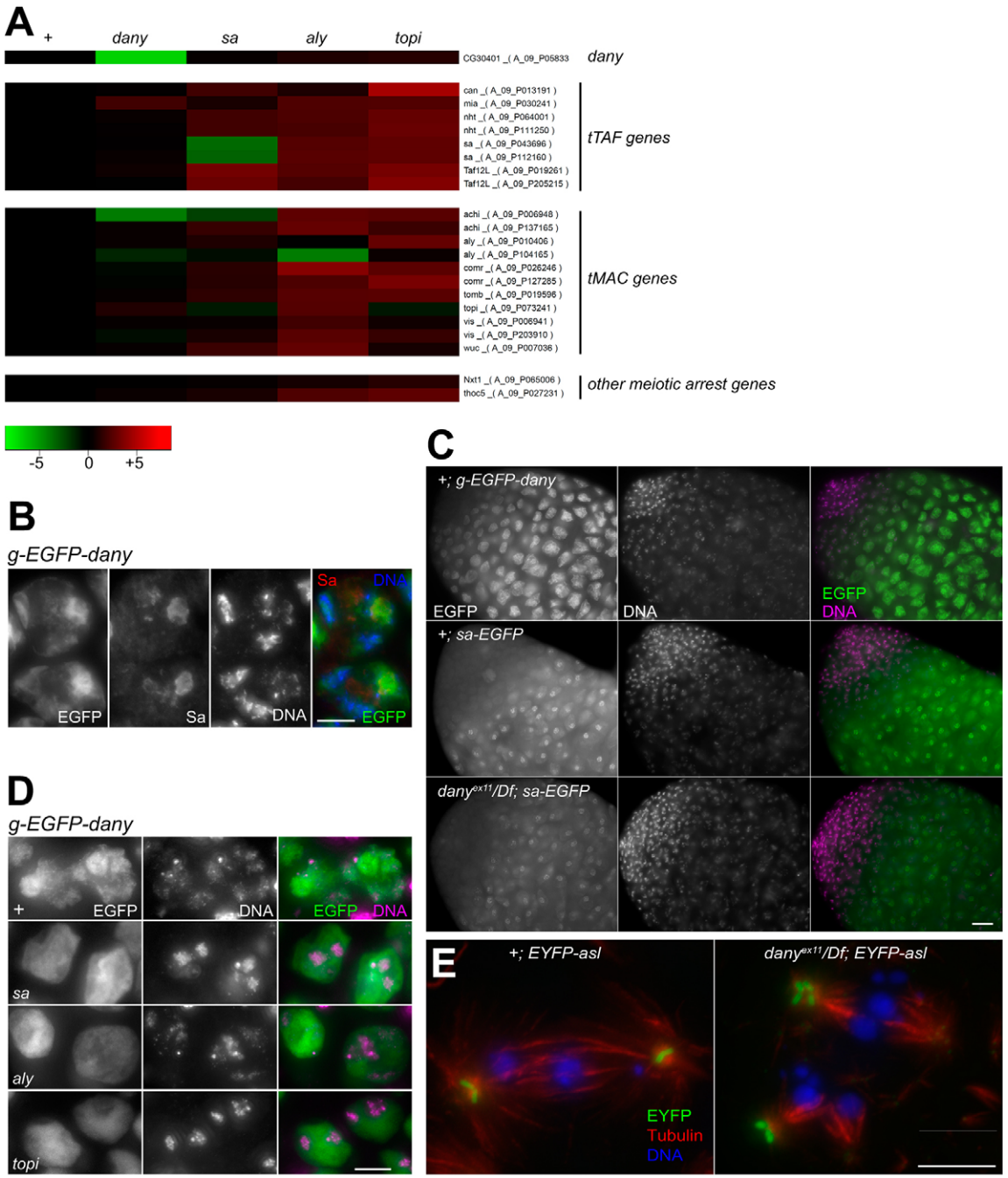

Fig. 5. *dany*, tTAF and tMAC genes do not cross-regulate each other. (A) Signals obtained with probes for *dany* or meiotic arrest genes on testis RNA samples from +/*Df(2R)BSC802* controls (+) were set to 1, and $\log_2$ transformed fold change in mutants lacking the function of the genes indicated at the top (*dany*, *sa*, *aly*, *topi*) is displayed as a heat map. Probe number (in brackets) and targeted gene are indicated to the right. (B) S5 spermatocytes from *g-EGFP-dany* testis after double labeling with anti-Sa and a DNA stain reveal that EGFP-Dany and the tTAF protein Sa are not strictly colocalized. (C) Distal testis regions from males carrying either *g-EGFP-dany* or *sa-EGFP* after DNA labeling reveal distinct behavior of Dany and Sa proteins. Nucleolar enrichment occurs already at the onset of Sa-EGFP expression in early spermatocytes but only in late spermatocytes in the case of EGFP-Dany. Moreover, Sa-EGFP behavior is not altered in *dany* mutants (*dany*^{ex11}/*Df(2R)BSC802*). (D) S5 spermatocytes from males expressing *g-EGFP-dany* in either wild-type (+) or the indicated mutant (*sa*, *aly*, *topi*) backgrounds after DNA labeling. (E) Meiotic cells from males expressing *EYFP-asl* in either a *dany*$^{+}$ (*dany*^{ex11}/*CyO*) or a *dany* mutant (*dany*^{ex11}/*Df(2R)BSC802*) background were identified after labeling with anti-α-Tubulin and a DNA stain. Meiotic cells are present but abnormal in *dany* mutants. Scale bars: 10 µm in B,D,E; 20 µm in C.

stage, the nuclear lamina in *sa*, *aly* and *topi* mutants was of wild-type appearance (Fig. 6A). During all subsequent stages (S4-S6), the intriguing difference in nuclear lamina appearance between *dany* mutants and controls was maintained (Fig. 6B; data not shown). At these later stages, nuclear lamina appearance in *sa*, *aly* and *topi* mutants was more similar to that in *dany* mutants, i.e. distinctly more balloon-like than in the controls (Fig. 6B). In conclusion, the first phenotypic abnormalities that we have been able to detect in *dany* mutants concern the association between chromatin and the nuclear envelope.

Development (2016) 143, 2664-2676 doi:10.1242/dev.134759

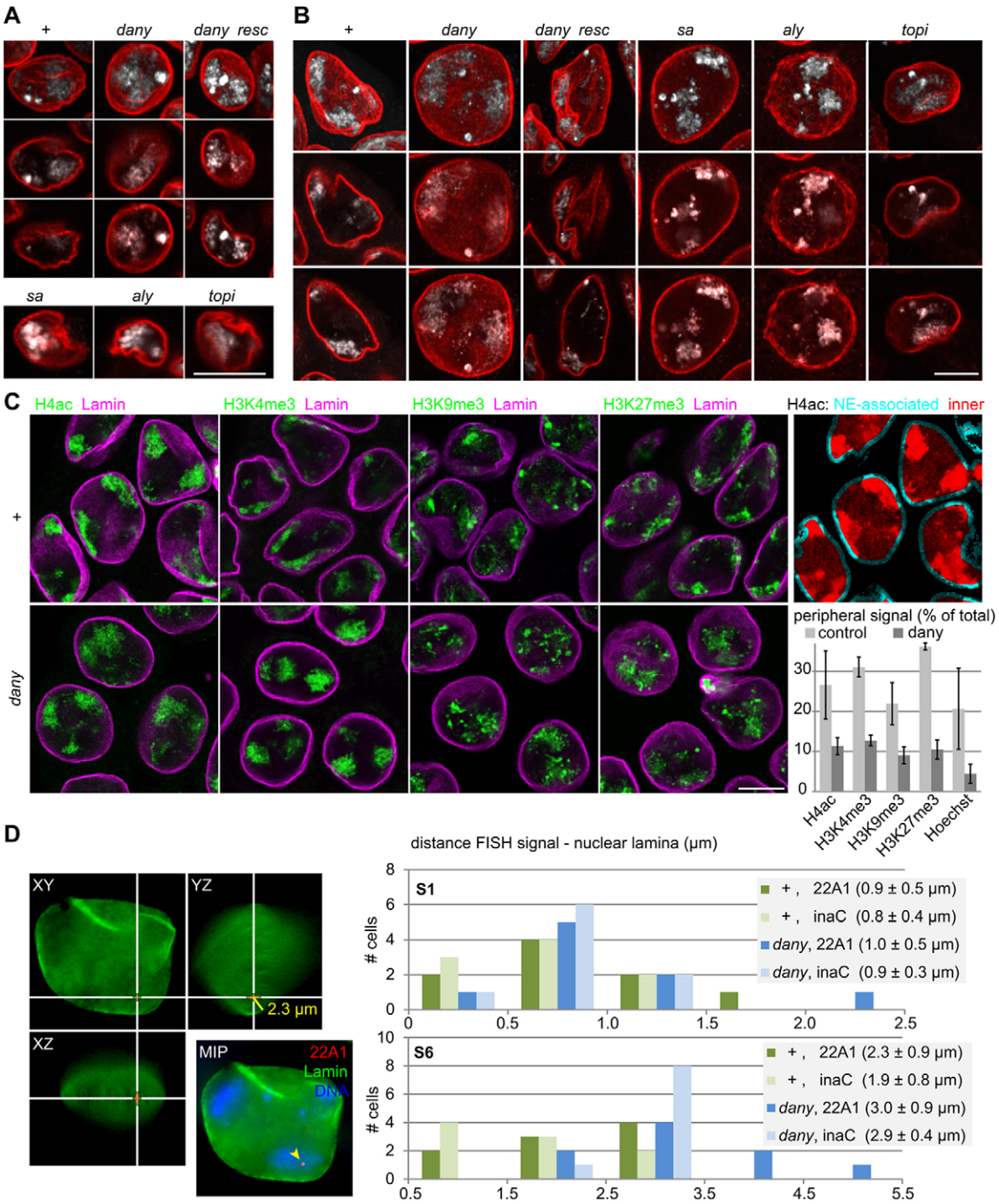

Fig. 6. Dany is required for nuclear shape distortion around chromosome territories. (A,B) Testis squash preparations were stained with anti-Lamin (red) and a DNA stain (gray) for the analysis of chromatin distribution and nuclear shape in spermatocytes at stages S3 (A) and S5 (B). Genotypes analyzed were *w* as control (+), $dany^{ex11}/Df(2R)BSC802$ without (*dany*) and with (*dany resc*) the *g-dany* transgene, sa^{1}/sa^{2} (*sa*), aly^{2}/aly^{5} (*aly*) and $topi^{Z3\text{-}0707}/topi^{Z3\text{-}2139}$ (*topi*). Maximum intensity projections are displayed in the top row. The next two rows present single focal planes through the nuclei shown at the top. Single focal sections are also presented in the bottom row in A. (C) Testes from *pUbi-EYFP-asl* control (+) and $dany^{ex11}/Df(2R)BSC802$ (*dany*) were squashed and stained together on the same slide with anti-Lamin and anti-modified histones (H4ac, H3K4me3, H3K9me3 and H3K27me3). Centrosomal EYFP-Asl fluorescence (not shown) was used for genotype identification. Single confocal sections through the equatorial region of S5/6 spermatocyte nuclei are shown. As illustrated in the upper right panel, the percentage of the anti-histone signal that was associated with the nuclear periphery (cyan region, NE) was determined. Average values are presented in the bar chart (±s.d.; *n*=3 cysts with 16 spermatocytes per cyst). Peripheral signals of DNA staining with Hoechst 33258 (not shown) were quantified as well. (D) Immuno-FISH was performed with testis squash preparations from control (+) and $dany^{ex11}/Df(2R)BSC802$ (*dany*) mutants using anti-Lamin, DNA staining and probes for either *inaC* or a cluster of testis-specific genes at 22A1. Image stacks were acquired. The *xy*-, *xz*- and *yz*-planes cutting through the FISH signal were viewed using Imaris, as illustrated in the micrographs. A maximum intensity projection (MIP) is shown of an S6 spermatocyte nucleus stack along the *z*-axis. The arrowhead indicates the 22A1 FISH signal. The shortest distances between FISH signals and the nuclear lamina were determined in S1 and S6 spermatocytes. All measurements are displayed in the histograms (*x*-axis: number of cells; *y*-axis: bins of the shortest distances between FISH signal and nuclear lamina with numbers indicating distance in µm at bin borders). Mean values (±s.d.) are given in the symbol legends. Three different cysts, and in each cyst three nuclei, were analyzed for each condition. Scale bars: 10 µm.

Development (2016) 143, 2664-2676 doi:10.1242/dev.134759

To assess whether loss of *dany* has any major effects on active and repressive chromatin marks, we compared the level and intranuclear localization of immunofluorescent signals in control and *dany* mutant spermatocytes after labeling with antibodies against modified histones: acetylated histone H4 (H4ac) and histone H3 with trimethylated K4 (H3K4me3), K9 (H3K9me3) or K27 (H3K27me3) (Fig. 6C). We could not detect any striking differences in global signal intensities between the *dany* mutant and control. However, these analyses clearly confirmed that association of chromatin with the nuclear envelope region is strongly reduced in *dany* mutant spermatocytes.

Intriguingly, the list of strongly derepressed genes in *dany* mutant testes contained a significantly higher number of genes strongly derepressed by Lam knockdown in the fat body (Chen et al., 2013) than expected stochastically (Table S1). For an initial evaluation of the effects of *dany* loss on intranuclear localization at the gene level by fluorescence *in situ* hybridization (FISH) to chromosomal DNA, *inaC* was selected as the gene most strongly derepressed in *dany* mutant testis according to our microarray data and as it is also associated with the nuclear lamina according to Lam-ID in Kc cells (Pickersgill et al., 2006), as well as strongly derepressed after Lam knockdown in fat body (Chen et al., 2013). In addition, we analyzed a testis-specific gene cluster at 22A1, which has been shown to be associated with the nuclear lamina in Kc cells and male germ cells during the early stages of spermatogenesis followed by relocalization into the nuclear interior in late spermatocytes (Pickersgill et al., 2006; Shevelyov et al., 2009). The genes within this cluster were at most mildly downregulated in *dany* mutant testis according to our microarray data. Immuno-FISH with anti-Lam and the *inaC* or the 22A1 FISH probe (Fig. 6D) indicated that both loci were preferentially close to the nuclear periphery in early spermatocytes (S1) in both control and *dany* mutants, as expected. In late control spermatocytes (S6), 22A1 tended to be farther away from the nuclear lamina, similar to previous reports (Shevelyov et al., 2009), whereas *inaC* was still relatively close to the nuclear periphery. Strikingly, compared with control, both loci were far more internal in *dany* mutant S6 spermatocytes, confirming that *dany* is required for normal chromatin association with the nuclear periphery.

DISCUSSION

Our identification and characterization of *dany* has uncovered a factor crucial for the realization of the spermatocyte-specific gene expression program in *Drosophila*. Loss of *dany* compromises the transcriptional activation of a large number of spermatocyte-specific genes and derepresses genes that are normally inactive in spermatocytes. Moreover, *dany* is required for normal association of spermatocyte chromatin with the nuclear periphery.

With regard to transcriptional activation, Dany is similar to tTAFs and tMAC. Mutations in tMAC genes have a severe effect on spermatocyte-specific gene expression (Doggett et al., 2011; Lu et al., 2013) (Fig. 4). In the case of tTAF mutants, fewer genes are affected and the reduction in transcript levels is often less severe. Loss of *dany* has even slightly milder effects, but there are still ~1000 genes with significantly reduced transcript levels. Many of these genes are also dependent on tMAC and tTAFs.

The fact that Dany is just as important for silencing of non-spermatocyte genes as for activation of spermatocyte-specific genes indicates that this protein does not function like the activators tTAFs and tMAC, which have not been implicated in gene silencing. Several additional observations support our conclusion. Dany intracellular localization in early spermatocytes is distinct from that of the tTAF Sa (Fig. 5C). *dany* transcript and protein levels depend neither on Sa nor on the tMAC components Aly and Topi (Fig. 5A,D). Vice versa, mutations in *dany* affect neither transcript levels of tTAF and tMAC genes (Fig. 5A) nor accumulation and intracellular localization of representative protein products (Sa and Can; Fig. 5C, Fig. S4).

dany orthologs cannot be detected outside the genus *Drosophila*, whereas the primordial *dan/danr* genes are present throughout the insect lineage. The testis-specific tMAC and tTAF genes are comparably young in evolutionary terms. The fact that several functionally independent factors of paramount importance for the highly complex spermatocyte-specific gene expression program have a recent origin provides further testimony of the surprising evolutionary dynamics of genes that function in the male germline. After a gene duplication event, *dany* has evolved to control the expression of thousands of genes in the male germline. Dany is a potent regulator; ectopic expression of *dany* in somatic tissues is highly toxic.

How does Dany exert its function? We demonstrate that Dany is a nuclear protein. After ectopic expression in larval salivary glands, it binds preferentially to all euchromatic interband regions of polytene chromosomes. In maturing spermatocytes, where it is normally expressed, Dany also appears to associate preferentially with euchromatic regions within chromosome territories and not with the regions of maximal DNA staining intensity corresponding to pericentromeric heterochromatin. As the Psq motif of some other proteins, including CENPB and transposases, is involved in sequence-specific DNA binding, it is conceivable that Dany and its closest relatives Dan and Danr bind to DNA as well. The Psq domain structure of Dan as revealed by NMR [Protein Data Bank (PDB) code 2ELH] is highly similar to that observed by X-ray crystallography in CENPB (PDB code 1HLV) (Tanaka et al., 2001). However, the DNA-binding region within CENPB is not restricted to the Psq motif but includes an additional helix-turn-helix domain that is not present in Dan, Danr and Dany. Similarly, the DNA-binding region of transposases extends considerably beyond the Psq motif. By mutating three amino acid codons within the Dany Psq motif, which correspond to positions contacting bound DNA in the case of CENPB, we were able to demonstrate the functional importance of this motif. However, Dany^{AAA} still retains some function; it promotes spermatogenesis beyond the stage when *dany* null mutant spermatocytes arrest. Moreover, the intracellular localization of Dany^{AAA} in spermatocytes appears to be normal. Additional analyses will be required to resolve whether the Psq motif of Dany indeed binds DNA. We point out that the Psq motif in CENPB contacts only four base pairs (Tanaka et al., 2001). Such a limited DNA sequence specificity could not explain the observed preferential association of Dany with euchromatic regions. Additional factors will have to be identified.

Interestingly, the first phenotypic abnormalities that we have detected in *dany* mutants occur in young spermatocytes soon after the onset of *dany* expression. Whereas chromosome territories tend to become enwrapped in the nuclear envelope when they are formed in wild-type spermatocytes during the S3 stage (Cenci et al., 1994; Fuller, 1993), *dany* mutant spermatocytes are devoid of such characteristic nuclear envelope deformations at the corresponding stage (Fig. 6). Thus, Dany appears to be required for normal chromatin association with the nuclear envelope. Since Dany is not enriched at the nuclear periphery, it obviously is very unlikely to function as a factor that directly establishes physical contact between chromatin and the nuclear envelope. But the extensive chromatin reorganization, which presumably occurs in early spermatocytes when thousands of previously repressed genes

Development (2016) 143, 2664-2676 doi:10.1242/dev.134759

become active while precursor-specific genes are inactivated, might be abnormal in the absence of *dany*. Thereby, chromatin properties that normally cause localization to the nuclear periphery might also be affected.

Dany's closest relatives Dan and Danr, which act partially redundantly in somatic tissues (Curtiss et al., 2007; Emerald et al., 2003; Kohwi et al., 2011, 2013), are crucial for the control of intranuclear position and silencing of the *hunchback* (*hb*) genomic locus in neuroblasts during embryogenesis (Kohwi et al., 2013). *hb* relocalization to the nuclear lamina, which is correlated with *hb* silencing and termination of Hb response competence, depends on timely Dan downregulation.

Changes in the association of genes with the nuclear periphery have previously been implicated in the control of the spermatocyte-specific gene expression program in *Drosophila*. In cell types other than spermatocytes, most spermatocyte-specific genes appear to be packaged into a repressive type of heterochromatin designated 'BLACK' heterochromatin, which is associated with Lam at the nuclear envelope (El-Sharnouby et al., 2013; Filion et al., 2010; Shevelyov et al., 2009; van Bemmel et al., 2013). In case of two representative testis-specific gene clusters (at 60D1 and 22A1), loss of Lam was shown to result in their derepression in somatic larval and cultured cells, and the normal transcriptional activation was accompanied by cluster repositioning into the nuclear interior of late spermatocytes (Shevelyov et al., 2009). Our immuno-FISH analyses support the notion that a repressive chromatin type that is normally associated with the nuclear periphery is impaired in *dany* mutants. The derepression of the eye-specific *inaC* gene in *dany* mutant spermatocytes was accompanied by delocalization away from the nuclear periphery into the interior. Extensive future work will be required to clarify the molecular basis and functional significance of our initial observations.

Even if an extensive correlation between intranuclear position and transcriptional activity were established by systematic studies, it remains to be considered whether loss of *dany* might affect the organization of chromatin within the nucleus indirectly. *dany* mutations could alter the expression program of particular chromatin regulators or proteins of the nuclear periphery. Indeed, some important chromatin regulators and nuclear envelope proteins have been shown to undergo drastic changes in expression levels during normal spermatogenesis. Su(Hw), a multi-zinc finger DNA-binding protein that can function as a transcriptional insulator and modulator of chromatin association with the nuclear lamina (Soshnev et al., 2013; van Bemmel et al., 2010), and the PRC2 complex components E(z) and Su(z) (Chen et al., 2011) are strongly downregulated in early spermatocytes, whereas Lamin C (LamC) expression is induced (Chen et al., 2013). However, in these particular cases, we did not detect an abnormal expression program in *dany* mutant testis by immunolabeling (data not shown).

We point out that loss of *dany* also results in the derepression of genes that appear to be Pc targets. Such genes are primarily within 'BLUE' heterochromatin (Filion et al., 2010). Pc-mediated repression of spermatocyte-specific genes has been proposed to be counteracted in spermatocytes by the combined action of tMAC and tTAFs. Although not identical, the *dany* mutant phenotype shares similarities with the meiotic arrest phenotype caused by loss of tMAC and tTAF function. Future work will be required to clarify the functional interactions between Dany and these major activators of spermatocyte-specific genes.

Extensive spatial intranuclear chromatin reorganization might guide many differentiation processes in complex eukaryotes. For example, hundreds of genes were reported to move towards or from the nuclear envelope during differentiation of mouse embryonic stem cells, concomitant with reduced or increased expression, respectively (Peric-Hupkes et al., 2010). Similar observations were made during adipogenic cell differentiation (Lund et al., 2013). Our identification and initial characterization of *dany* should help support future progress towards a molecular understanding of the mechanisms that coordinate change in spatial genome organization and cell type-specific expression programs.

MATERIALS AND METHODS

Drosophila strains

The transposon insertion *P{GSV7}GS22077* (DGRC #203614) (Toba et al., 1999) was used for the isolation of the imprecise excision events $dany^{ex4}$, $dany^{ex11}$ and $dany^{ex83}$ as described in the supplementary Materials and Methods. *Df(2R)BSC802* (Cook et al., 2012) [Bloomington *Drosophila* Stock Center (BDSC) #27374] deletes the *dany* gene.

Plasmid constructs used for the generation of transgenic lines are described in detail in the supplementary Materials and Methods. Lines for GAL4-regulated transgenic RNAi, *UAS-V20dany*^{shmiR17} and *UAS-W20dany*^{shmiR41} were generated after integration of the constructs pVALIUM20-*dany*^{shmiR17} and pWALIUM20-*dany*^{shmiR41} into the attP2 landing site (Groth et al., 2004).

Lines with transgenes under control of the *dany* cis-regulatory region (*g-dany*, *g-EGFP-dany*, *g-dany-EGFP*, *g-dany*^{AAA}*-EGFP*) were obtained after integration (BestGene) of pattB constructs (Bischof et al., 2013) into the attP40 landing site (Markstein et al., 2008). For analysis of transgene expression and function in *dany* mutants they were recombined with $dany^{ex11}$ and the recombinant chromosome was crossed over *Df(2R)BSC802*. We obtained indistinguishable results after recombination of the transgenes with the deficiency, followed by crossing the recombinant chromosome over the *dany* allele.

Transgenic lines allowing GAL4-regulated expression of *dany* with or without EGFP extension (*UASt-dany*, *UASt-EGFP-dany*, *UASt-dany-EGFP*) were obtained with pUASt constructs after microinjection into w^{1118} (BestGene). Multiple independent insertions were established and analyzed. The driver lines *bam-GAL4-VP16* (Chen and McKearin, 2003) and *esg-GAL4 (P{PZ}esg[05730] P{GawB}05730B), P{w{+mC}=tubPGAL80TS}20* (Keisman et al., 2001; McGuire et al., 2003) have been described. The experiments involving temporally regulated expression in the salivary gland were performed with *P{w*$^{+}$*, UASt-EGFP-dany}*III.1.

The following alleles of meiotic arrest mutants were used in heteroallelic combinations: sa^{1} and sa^{2} (Hiller et al., 2004) (kindly provided by M. Fuller, Stanford University, CA, USA), aly^{2} and aly^{5} (White-Cooper et al., 2000) (kindly provided by H. White-Cooper, Cardiff University, UK), $topi^{Z3\text{-}0707}$ (BDSC #38441) and $topi^{Z3\text{-}2139}$ (BDSC #38442) (Perezgasga et al., 2004). For the analysis of *g-EGFP-dany* expression in these meiotic arrest mutants, we used testis from heteroallelic mutants carrying one copy of the transgene.

Strains with the transgenes *can-6myc* (X) (Chen et al., 2005) and *sa-EGFP* (X) (Chen et al., 2005) were kindly provided by M. Fuller, *Pc-EGFP* (III) (Dietzel et al., 1999) by R. Paro (ETHZ, Basel, Switzerland) and *pUbi-EYFP-asl* (X) (Rebollo et al., 2007) by C. Gonzalez (IRB, Barcelona, Spain). The expression of these transgenes was analyzed in testis isolated from $dany^{ex11}$/*Df(2R)BSC802* males carrying one copy of a given transgene.

Primers used in plasmid construction and analysis of genomic DNA by PCR are listed in Table S2.

Fertility tests

Five to ten males of the genotype to be tested were crossed individually, each with three tester virgins. The tester strain was *w*. For analysis of female fertility, three virgin females of the genotype to be tested were pooled and crossed with three tester males. Five replicate crosses were set up per genotype for female fertility determination. Two days after setting up the crosses, flies were transferred to a fresh vial and discarded 48 h later. Adult progeny flies that eclosed in the vial were counted. For the control genotype *Df(2R)BSC802*/+ we obtained on average 217 progeny flies from a single male and 232 from three females.

Development (2016) 143, 2664-2676 doi:10.1242/dev.134759

Microscopy analyses

For whole-mount testis preparations, dissection was performed in testis buffer (183 mM KCl, 47 mM NaCl, 10 mM Tris-HCl, pH 6.8). Testes were fixed in depression slides for 10 min in PBS containing 4% formaldehyde and 0.1% Triton X-100. For DNA staining, testes were incubated for 10 min in PBS, 0.1% Triton X-100 (PBTx) containing 1 µg/ml Hoechst 33258. After three washes with PBS, testes were transferred to a drop of mounting medium (70% glycerol, 1% n-propyl gallate, 0.05% p-phenylenediamine) on a slide before adding a coverslip.

Testis squash preparations were made and stained essentially as described previously (White-Cooper, 2004), according to protocol 3.3.2, except that we used the mounting medium described above. For accurate comparison of signal intensities obtained with the antibodies against modified histones (H4ac, H3K4me3, H3K9me3, H3K27me3) in *dany* mutant and control spermatocytes, we used *pUbi-EYFP-asl* males for isolation of control testes and mixed these with *dany* mutant testes before squashing, fixation and staining on the same slide. After imaging with constant settings, control and *dany* mutant spermatocytes were identified based on the presence and absence of EYFP-Asl, respectively.

For inactivation of GAL80^{ts}, we transferred third instar wandering stage larvae grown at 18°C onto apple juice agar plates, which were then floated on a 29°C water bath for 4 h before dissection and staining of salivary glands as described (Radermacher et al., 2014).

Detailed information on antibodies is provided in the supplementary Materials and Methods. Images were acquired using a Zeiss Cell Observer HS wide-field microscope, except for those in Fig. 6A-C for which we used an Olympus FluoView 1000 laser-scanning confocal microscope. Single focal planes were captured with a 10× objective when imaging entire testes. *z*-stacks were acquired with 40×/0.75, 60×/1.42 or 63×/1.4 objectives for analysis of testis subregions at high resolution. Maximum intensity projections were generated using AxioVision (Zeiss) for wide-field images and Imaris (Bitplane) for confocal images. For the images in Fig. 3D, *z*-stacks of five focal planes with 250 nm spacing were acquired with a 100×/1.4 objective and deconvolved (Huygens Professional software) before maximum intensity projection (ImageJ).

ImageJ was used for estimating the fraction of intranuclear immunofluorescent signal that was close to the nuclear envelope in the testis squash preparations. Image stacks of well-squashed cysts with sixteen spermatocytes in a monolayer were imaged with the laser-scanning confocal microscope. First, the focal plane within an image stack which contained a maximum number of equatorial sections through spermatocyte nuclei was selected manually. The anti-Lam signal was then used for image segmentation. Signal intensity obtained with the antibody against a particular modified histone (H4ac, H3K4me3, H3K9me3 or H3K37me3) within the regions confined by the rims of anti-Lam signal was integrated (total nuclear anti-histone signal). After shrinkage of the measured region by 10 pixels (length of one pixel=103 nm), signal intensity in the anti-histone channel was again integrated (internal nuclear anti-histone signal). Subtraction of the internal from the total nuclear signal yielded the nuclear envelope-associated anti-histone signal. The nuclear envelope-associated signal was converted into percent of total nuclear signal. For each genotype and anti-histone antibody, this percentage was determined for each of three independent image stacks followed by averaging. A *t*-test was performed for analysis of statistical differences between the average observed in control and *dany* mutants, respectively. The finding that the average percentage of nuclear envelope-associated anti-histone signal is consistently larger in control than *dany* mutant spermatocytes was also observed when the nuclear region was shrunk by a pixel value other than 10 (5, 15 or 20 pixels) and when the analysis was extended to include all focal planes of the image stack.

Immuno-FISH was performed essentially as described (Blattner et al., 2016). Anti-Lam and anti-LamC were used as a mixture. FISH probes were generated as described (Dernburg, 2011). The fosmid FF031161 (Ejsmont et al., 2009) was used for preparation of the 22A1 gene cluster probe, and pooled PCR products amplified with primers AB168-AB177 (Table S2) from *w* genomic DNA for the *inaC* probe. ChromaTide Alexa Fluor 568-5-dUTP (Thermo Fisher Scientific) was used for probe labeling. The denaturation step was performed at 95°C for 3 min and hybridization for 18 h at 30°C. Slides were washed twice in 50% formamide, 2×SSCT at 30°C for 1 h each. Thereafter, additional washes were performed at room temperature in 25% formamide, 2×SSCT for 10 min and three times in 2×SSCT for 10 min each. DNA staining and mounting were performed as described above. Image stacks with 250 nm spacing between focal planes were acquired with a 63×/1.4 oil-immersion objective on a Zeiss Cell Observer HS microscope. Imaris 'section view' was used for analysis of the shortest distance between the FISH signal and the nuclear lamina.

Expression profiling

Total RNA was isolated from testes dissected from young adult males (0-2 days after eclosion). Five genotypes were analyzed: (1) w^{1118}/Y; *Df(2R)BSC802*/+, (2) w^{1118}/Y; *Df(2R)BSC802*/*dany*^{ex11}, (3) *w*/Y; aly*^{2} *red e*/*aly*^{5} *red e*, (4) *+/Y; bw; topi*$^{Z3\text{-}0707}$/*topi*$^{Z3\text{-}2139}$ and (5) *+/Y;th sa*^{1} *red/ru h sa*^{2} *ca*. After dissection of 20 testes, these were transferred into 5 µl ice-cold testis buffer, snap frozen in liquid nitrogen and stored at −80°C. Eighty testes per genotype were pooled for extraction of total RNA with Trizol (Ambion). RNA was resuspended in 10 µl DEPC-treated water before digestion of residual DNA (DNA-Free Kit, Ambion). Four independent RNA samples were prepared and analyzed from genotype 1, three from genotype 2, and two for genotypes 2-5. RNA samples were used for the generation of Cy3-labeled cRNA (Low RNA Input Linear Amplification Kit, Agilent Technologies) and hybridization to *Drosophila* gene expression microarrays (4×44 K microarrays, G2519F-021791, Agilent Technologies). Before hybridization, cRNA was purified (Absolutely RNA Nanoprep Kit, Agilent Technologies). A NanoDrop 2000 spectrophotometer (Thermo Scientific) was used for quantification, a 2100 Bioanalyzer (Agilent Technologies) for quality control, and Agilent Feature Extraction software for quantification of signal intensities.

Data were processed and analyzed using R (v3.0.2) and the Limma package (Ritchie et al., 2015; Smyth, 2005). The normexp convolution method was used for background correction. Corrected signal intensities were quantile normalized. Signal intensities observed with technical replicate probes present more than once on the microarray were averaged. Probes with low signals were filtered out from the total of 32,162 probes. 27,005 probes with a signal ≥5.8 ($\log_2$ transformed intensity value) on at least two microarrays were retained for further analyses. Hierarchical clustering was performed for the comparison of all the different hybridizations. A two-group analysis was performed for the comparison of *+/Df(2R)BSC802* and *dany*^{ex11}/*Df(2R)BSC802*, and an ANOVA for the comparison of *dany* and meiotic arrest mutants (*sa*, *aly*, *topi*). Probes were only considered to have differential signal intensities if the associated false discovery rate (FDR)-corrected *P*-value was less than 0.05. FlyMine (http://www.flymine.org/) (Lyne et al., 2007) was used for the analysis of tissue specificity of genes that were upregulated or downregulated in *dany* mutants. Microarray data are available at GEO (accession number GSE76298).

Acknowledgements

We thank Konrad Basler, Minx Fuller, Pamela Geyer, Cayetano Gonzalez, Rick Jones, Jürg Müller, Renato Paro and Helen White-Cooper for providing fly strains and/or antibodies; Norbert Perrimon for vector plasmids; Rita Lecca and the Functional Genomics Center Zurich for supporting the microarray hybridizations; Charity Law, Helen Lindsay and Mark Robinson for assisting during the microarray data analysis; and Emmanuel Caussinus for assisting during immunofluorescent signal quantification.

Competing interests

The authors declare no competing or financial interests.

Author contributions

M.T. and A.C.B. performed all experiments except microarray hybridizations, analyzed data, designed the experiments together with C.F.L. and contributed to manuscript writing. S.L. performed microarray hybridizations and bioinformatic analysis of the transcriptome data. C.F.L. conceived and supervised the study, analyzed data and wrote the manuscript.

Funding

This work was supported by the Swiss National Science Foundation (Schweizerischer Nationalfonds zur Förderung der Wissenschaftlichen Forschung) [grant 31003A_120276 to C.F.L.].

Development (2016) 143, 2664-2676 doi:10.1242/dev.134759

Data availability

Microarray data are available at Gene Expression Omnibus under accession number GSE76298.

Supplementary information

Supplementary information available online at
http://dev.biologists.org/lookup/doi/10.1242/dev.134759.supplemental

References

Andrews, J., Bouffard, G. G., Cheadle, C., Lü, J., Becker, K. G. and Oliver, B. (2000). Gene discovery using computational and microarray analysis of transcription in the Drosophila melanogaster testis. *Genome Res.* **10**, 2030-2043.

Ayyar, S., Jiang, J., Collu, A., White-Cooper, H. and White, R. A. (2003). Drosophila TGIF is essential for developmentally regulated transcription in spermatogenesis. *Development* **130**, 2841-2852.

Beall, E. L., Lewis, P. W., Bell, M., Rocha, M., Jones, D. L. and Botchan, M. R. (2007). Discovery of tMAC: a Drosophila testis-specific meiotic arrest complex paralogous to Myb-Muv B. *Genes Dev.* **21**, 904-919.

Bischof, J., Bjorklund, M., Furger, E., Schertel, C., Taipale, J. and Basler, K. (2013). A versatile platform for creating a comprehensive UAS-ORFeome library in Drosophila. *Development* **140**, 2434-2442.

Blattner, A. C., Chaurasia, S., McKee, B. D. and Lehner, C. F. (2016). Separase is required for homolog and sister disjunction during Drosophila melanogaster male meiosis, but not for biorientation of sister centromeres. *PLoS Genet.* **12**, e1005996.

Brown, J. B., Boley, N., Eisman, R., May, G. E., Stoiber, M. H., Duff, M. O., Booth, B. W., Wen, J., Park, S., Suzuki, A. M. et al. (2014). Diversity and dynamics of the Drosophila transcriptome. *Nature* **512**, 393-399.

Cenci, G., Bonaccorsi, S., Pisano, C., Verni, F. and Gatti, M. (1994). Chromatin and microtubule organization during premeiotic, meiotic and early postmeiotic stages of Drosophila- melanogaster spermatogenesis. *J. Cell Sci.* **107**, 3521-3534.

Chen, D. and McKearin, D. M. (2003). A discrete transcriptional silencer in the bam gene determines asymmetric division of the Drosophila germline stem cell. *Development* **130**, 1159-1170.

Chen, X., Hiller, M., Sancak, Y. and Fuller, M. T. (2005). Tissue-specific TAFs counteract Polycomb to turn on terminal differentiation. *Science* **310**, 869-872.

Chen, X., Lu, C., Morillo Prado, J. R., Eun, S. H. and Fuller, M. T. (2011). Sequential changes at differentiation gene promoters as they become active in a stem cell lineage. *Development* **138**, 2441-2450.

Chen, H., Chen, X. and Zheng, Y. (2013). The nuclear lamina regulates germline stem cell niche organization via modulation of EGFR signaling. *Cell Stem Cell* **13**, 73-86.

Chintapalli, V. R., Wang, J. and Dow, J. A. (2007). Using FlyAtlas to identify better Drosophila melanogaster models of human disease. *Nat. Genet.* **39**, 715-720.

Cook, R. K., Christensen, S. J., Deal, J. A., Coburn, R. A., Deal, M. E., Gresens, J. M., Kaufman, T. C. and Cook, K. R. (2012). The generation of chromosomal deletions to provide extensive coverage and subdivision of the Drosophila melanogaster genome. *Genome Biol.* **13**, R21.

Curtiss, J., Burnett, M. and Mlodzik, M. (2007). distal antenna and distal antenna-related function in the retinal determination network during eye development in Drosophila. *Dev. Biol.* **306**, 685-702.

Dernburg, A. F. (2011). Fragmentation and labeling of probe DNA for whole-mount FISH in Drosophila. *Cold Spring Harb. Protoc.* **2011**, 1527-1530.

Dietzel, S., Niemann, H., Bruckner, B., Maurange, C. and Paro, R. (1999). The nuclear distribution of Polycomb during Drosophila melanogaster development shown with a GFP fusion protein. *Chromosoma* **108**, 83-94.

Doggett, K., Jiang, J., Aleti, G. and White-Cooper, H. (2011). Wake-up-call, a lin-52 paralogue, and Always early, a lin-9 homologue physically interact, but have opposing functions in regulating testis-specific gene expression. *Dev. Biol.* **355**, 381-393.

Dorus, S., Busby, S. A., Gerike, U., Shabanowitz, J., Hunt, D. F. and Karr, T. L. (2006). Genomic and functional evolution of the Drosophila melanogaster sperm proteome. *Nat. Genet.* **38**, 1440-1445.

Ejsmont, R. K., Sarov, M., Winkler, S., Lipinski, K. A. and Tomancak, P. (2009). A toolkit for high-throughput, cross-species gene engineering in Drosophila. *Nat. Methods* **6**, 435-437.

El-Sharnouby, S., Redhouse, J. and White, R. A. H. (2013). Genome-wide and cell-specific epigenetic analysis challenges the role of polycomb in Drosophila spermatogenesis. *PLoS Genet.* **9**, e1003842.

Emerald, B. S., Curtiss, J., Mlodzik, M. and Cohen, S. M. (2003). Distal antenna and distal antenna related encode nuclear proteins containing pipsqueak motifs involved in antenna development in Drosophila. *Development* **130**, 1171-1180.

Filion, G. J., van Bemmel, J. G., Braunschweig, U., Talhout, W., Kind, J., Ward, L. D., Brugman, W., de Castro, I. J., Kerkhoven, R. M., Bussemaker, H. J. et al. (2010). Systematic protein location mapping reveals five principal chromatin types in Drosophila cells. *Cell* **143**, 212-224.

Fuller, M. T. (1993). Spermatogenesis. In *The Development of Drosophila melanogaster* (ed. M. Bate and A. Martinez Arias), pp. 71-148. Cold Spring Harbor, NY: Cold Spring Harbor Laboratory Press.

Gan, Q., Chepelev, I., Wei, G., Tarayrah, L., Cui, K., Zhao, K. and Chen, X. (2010). Dynamic regulation of alternative splicing and chromatin structure in Drosophila gonads revealed by RNA-seq. *Cell Res.* **20**, 763-783.

Graveley, B. R., Brooks, A. N., Carlson, J. W., Duff, M. O., Landolin, J. M., Yang, L., Artieri, C. G., van Baren, M. J., Boley, N., Booth, B. W. et al. (2011). The developmental transcriptome of Drosophila melanogaster. *Nature* **471**, 473-479.

Groth, A. C., Fish, M., Nusse, R. and Calos, M. P. (2004). Construction of transgenic Drosophila by using the site-specific integrase from phage phiC31. *Genetics* **166**, 1775-1782.

Hiller, M., Chen, X., Pringle, M. J., Suchorolski, M., Sancak, Y., Viswanathan, S., Bolival, B., Lin, T.-Y., Marino, S. and Fuller, M. T. (2004). Testis-specific TAF homologs collaborate to control a tissue-specific transcription program. *Development* **131**, 5297-5308.

Jiang, J. and White-Cooper, H. (2003). Transcriptional activation in Drosophila spermatogenesis involves the mutually dependent function of aly and a novel meiotic arrest gene cookie monster. *Development* **130**, 563-573.

Jiang, J., Benson, E., Bausek, N., Doggett, K. and White-Cooper, H. (2007). Tombola, a tesmin/TSO1-family protein, regulates transcriptional activation in the Drosophila male germline and physically interacts with always early. *Development* **134**, 1549-1559.

Keisman, E. L., Christiansen, A. E. and Baker, B. S. (2001). The sex determination gene doublesex regulates the A/P organizer to direct sex-specific patterns of growth in the Drosophila genital imaginal disc. *Dev. Cell* **1**, 215-225.

Kohwi, M., Hiebert, L. S. and Doe, C. Q. (2011). The pipsqueak-domain proteins Distal antenna and Distal antenna-related restrict Hunchback neuroblast expression and early-born neuronal identity. *Development* **138**, 1727-1735.

Kohwi, M., Lupton, J. R., Lai, S.-L., Miller, M. R. and Doe, C. Q. (2013). Developmentally regulated subnuclear genome reorganization restricts neural progenitor competence in Drosophila. *Cell* **152**, 97-108.

Li, V. C., Davis, J. C., Lenkov, K., Bolival, B., Fuller, M. T. and Petrov, D. A. (2009). Molecular evolution of the testis TAFs of Drosophila. *Mol. Biol. Evol.* **26**, 1103-1116.

Lin, T. Y., Viswanathan, S., Wood, C., Wilson, P. G., Wolf, N. and Fuller, M. T. (1996). Coordinate developmental control of the meiotic cell-cycle and spermatid differentiation in Drosophila males. *Development* **122**, 1331-1341.

Lu, C. and Fuller, M. T. (2015). Recruitment of mediator complex by cell type and stage-specific factors required for tissue-specific TAF dependent gene activation in an adult stem cell lineage. *PLoS Genet.* **11**, e1005701.

Lu, C., Kim, J. and Fuller, M. T. (2013). The polyubiquitin gene Ubi-p63E is essential for male meiotic cell cycle progression and germ cell differentiation in Drosophila. *Development* **140**, 3522-3531.

Lund, E., Oldenburg, A. R., Delbarre, E., Freberg, C. T., Duband-Goulet, I., Eskeland, R., Buendia, B. and Collas, P. (2013). Lamin A/C-promoter interactions specify chromatin state-dependent transcription outcomes. *Genome Res.* **23**, 1580-1589.

Lyne, R., Smith, R., Rutherford, K., Wakeling, M., Varley, A., Guillier, F., Janssens, H., Ji, W., McLaren, P., North, P. et al. (2007). FlyMine: an integrated database for Drosophila and Anopheles genomics. *Genome Biol.* **8**, R129.

Markstein, M., Pitsouli, C., Villalta, C., Celniker, S. E. and Perrimon, N. (2008). Exploiting position effects and the gypsy retrovirus insulator to engineer precisely expressed transgenes. *Nat. Genet.* **40**, 476-483.

McGuire, S. E., Le, P. T., Osborn, A. J., Matsumoto, K. and Davis, R. L. (2003). Spatiotemporal rescue of memory dysfunction in Drosophila. *Science* **302**, 1765-1768.

Parsch, J. and Ellegren, H. (2013). The evolutionary causes and consequences of sex-biased gene expression. *Nat. Rev. Genet.* **14**, 83-87.

Perezgasga, L., Jiang, J., Bolival, B., Jr., Hiller, M., Benson, E., Fuller, M. T. and White-Cooper, H. (2004). Regulation of transcription of meiotic cell cycle and terminal differentiation genes by the testis-specific Zn-finger protein matotopetli. *Development* **131**, 1691-1702.

Peric-Hupkes, D., Meuleman, W., Pagie, L., Bruggeman, S. W. M., Solovei, I., Brugman, W., Graf, S., Flicek, P., Kerkhoven, R. M., van Lohuizen, M. et al. (2010). Molecular maps of the reorganization of genome-nuclear lamina interactions during differentiation. *Mol. Cell* **38**, 603-613.

Pickersgill, H., Kalverda, B., de Wit, E., Talhout, W., Fornerod, M. and van Steensel, B. (2006). Characterization of the Drosophila melanogaster genome at the nuclear lamina. *Nat. Genet.* **38**, 1005-1014.

Radermacher, P. T., Myachina, F., Bosshardt, F., Pandey, R., Mariappa, D., Muller, H.-A. J. and Lehner, C. F. (2014). O-GlcNAc reports ambient temperature and confers heat resistance on ectotherm development. *Proc. Natl. Acad. Sci. USA* **111**, 5592-5597.

Rebollo, E., Sampaio, P., Januschke, J., Llamazares, S., Varmark, H. and Gonzalez, C. (2007). Functionally unequal centrosomes drive spindle orientation in asymmetrically dividing Drosophila neural stem cells. *Dev. Cell* **12**, 467-474.

Ritchie, M. E., Phipson, B., Wu, D., Hu, Y., Law, C. W., Shi, W. and Smyth, G. K. (2015). limma powers differential expression analyses for RNA-sequencing and microarray studies. *Nucleic Acids Res.* **43**, e47.

Development (2016) 143, 2664-2676 doi:10.1242/dev.134759

Sadasivam, S. and DeCaprio, J. A. (2013). The DREAM complex: master coordinator of cell cycle-dependent gene expression. *Nat. Rev. Cancer* **13**, 585-595.

Shevelyov, Y. Y., Lavrov, S. A., Mikhaylova, L. M., Nurminsky, I. D., Kulathinal, R. J., Egorova, K. S., Rozovsky, Y. M. and Nurminsky, D. I. (2009). The B-type lamin is required for somatic repression of testis-specific gene clusters. *Proc. Natl. Acad. Sci. USA* **106**, 3282-3287.

Siegmund, T. and Lehmann, M. (2002). The Drosophila Pipsqueak protein defines a new family of helix-turn-helix DNA-binding proteins. *Dev. Genes Evol.* **212**, 152-157.

Smyth, G. K. (2005). Limma: linear models for microarray data. In *Bioinformatics and Computational Biology Solutions using R and Bioconductor* (ed. R. Gentleman, V. Carey, S. Dudoit, R. Irizarry and W. Huber), pp. 397-420. New York: Springer.

Soshnev, A. A., Baxley, R. M., Manak, J. R., Tan, K. and Geyer, P. K. (2013). The insulator protein Suppressor of Hairy-wing is an essential transcriptional repressor in the Drosophila ovary. *Development* **140**, 3613-3623.

Steffen, P. A. and Ringrose, L. (2014). What are memories made of? How Polycomb and Trithorax proteins mediate epigenetic memory. *Nat. Rev. Mol. Cell Biol.* **15**, 340-356.

Tanaka, Y., Nureki, O., Kurumizaka, H., Fukai, S., Kawaguchi, S., Ikuta, M., Iwahara, J., Okazaki, T. and Yokoyama, S. (2001). Crystal structure of the CENP-B protein-DNA complex: the DNA-binding domains of CENP-B induce kinks in the CENP-B box DNA. *EMBO J.* **20**, 6612-6618.

Toba, G., Ohsako, T., Miyata, N., Ohtsuka, T., Seong, K. H. and Aigaki, T. (1999). The gene search system. A method for efficient detection and rapid molecular identification of genes in Drosophila melanogaster. *Genetics* **151**, 725-737.

van Bemmel, J. G., Pagie, L., Braunschweig, U., Brugman, W., Meuleman, W., Kerkhoven, R. M. and van Steensel, B. (2010). The insulator protein SU(HW) fine-tunes nuclear lamina interactions of the Drosophila genome. *PLoS ONE* **5**, e15013.

van Bemmel, J. G., Filion, G. J., Rosado, A., Talhout, W., de Haas, M., van Welsem, T., van Leeuwen, F. and van Steensel, B. (2013). A network model of the molecular organization of chromatin in Drosophila. *Mol. Cell* **49**, 759-771.

Vibranovski, M. D., Lopes, H. F., Karr, T. L. and Long, M. (2009). Stage-specific expression profiling of Drosophila spermatogenesis suggests that meiotic sex chromosome inactivation drives genomic relocation of testis-expressed genes. *PLoS Genet.* **5**, e1000731.

Wang, Z. and Mann, R. S. (2003). Requirement for two nearly identical TGIF-related homeobox genes in Drosophila spermatogenesis. *Development* **130**, 2853-2865.

White-Cooper, H. (2004). Spermatogenesis: analysis of meiosis and morphogenesis. *Methods Mol. Biol.* **247**, 45-75.

White-Cooper, H. (2010). Molecular mechanisms of gene regulation during Drosophila spermatogenesis. *Reproduction* **139**, 11-21.

White-Cooper, H. and Caporilli, S. (2013). Transcriptional and post-transcriptional regulation of Drosophila germline stem cells and their differentiating progeny. *Adv. Exp. Med. Biol.* **786**, 47-61.

White-Cooper, H., Leroy, D., MacQueen, A. and Fuller, M. T. (2000). Transcription of meiotic cell cycle and terminal differentiation genes depends on a conserved chromatin associated protein, whose nuclear localisation is regulated. *Development* **127**, 5463-5473.

Zhao, J., Klyne, G., Benson, E., Gudmannsdottir, E., White-Cooper, H. and Shotton, D. (2010). FlyTED: the drosophila testis gene expression database. *Nucleic Acids Res.* **38**, D710-D715.